HHS Public Access

Author manuscript

Seizure. Author manuscript; available in PMC 2019 January 01.

Published in final edited form as:

Seizure. 2018 January ; 54: 11–18. doi:10.1016/j.seizure.2017.11.004.

Quantification of Perivascular Spaces at 7 Tesla: A Potential MRI Biomarker for Epilepsy

Rebecca Emily Feldman, PhD[1,2], **Jack Rutland**[1,2], **Madeline Cara Fields, MD**[3], **Lara Vanessa Marcuse, MD**[3], **Puneet S Pawha, MD**[2], **Bradley Neil Delman, MD**[2], and **Priti Balchandani, PhD**[1,2]

[1]Translational and Molecular Imaging Institute, Icahn School of Medicine at Mount Sinai, New York, New York, United States

[2]Radiology, Icahn School of Medicine at Mount Sinai, New York, New York, United States

[3]Department of Neurology, Mount Sinai Hospital, New York, New York, United States

Abstract

Purpose—7 Tesla (7T) magnetic resonance imaging (MRI) facilitates the visualization of the brain with resolution and contrast beyond what is available at conventional clinical field strengths, enabling improved detection and quantification of small structural features such as perivascular spaces (PVSs). The distribution of PVSs, detected *in vivo* at 7T, may act as a biomarker for the effects of epilepsy. In this work, we systematically quantify the PVSs in the brains of epilepsy patients and compare them to healthy controls.

Methods—T_2-weighted turbo spin echo images were obtained at 7T on 21 epilepsy patients and 17 healthy controls. For all subjects, PVSs were manually marked on Osirix image analysis software. Marked PVSs with diameter ≥ 0.5 mm were then mapped by hemisphere and lobe. The asymmetry index (AI) was calculated for each region and the maximum asymmetry index ($|AI_{max}|$) was reported for each subject. The asymmetry in epilepsy subjects was compared to that of controls, and the region with highest asymmetry was compared to the suspected seizure onset zone.

Corresponding Author: Rebecca Feldman, PhD, Translational and Molecular Imaging Institute, Icahn School of Medicine at Mount Sinai, 1470 Madison Avenue; Floor 1, New York, NY 10129, rebecca.feldman2@mountsinai.org, Tel: 212-824-8471, Fax: 646-537-9589.

Disclosure of Conflicts of Interest

Dr. Balchandani has received support from NIH-NINDS R00 NS070821, NIH R01 MH109544; Icahn School of Medicine Capital Campaign, Translational and Molecular Imaging Institute and Department of Radiology, Icahn School of Medicine at Mount Sinai, Siemens Healthcare

Jack Rutland has received support from Health Resources and Services Administration Health Careers Opportunity Program: Northeast Regional Alliance MedPREP Program, Icahn School of Medicine at Mount Sinai Grant D18HP29036

The remaining authors do not have any conflict of interest to disclose

Results—There was a significant difference between the $|AI_{max}|$ in epilepsy subjects and in controls (p = 0.016). In 72% of patients, the region or lobe of the brain showing maximum PVS asymmetry was the same as the region containing the suspected seizure onset zone.

Conclusion—These findings suggest that epilepsy may be associated with significantly asymmetric distribution of PVSs in the brain. Furthermore, the region of maximal asymmetry of the PVSs may help provide localization or confirmation of the seizure onset zone.

Introduction

Ultra-high field magnetic resonance imaging (MRI) scanners, such as those operating at 7 Tesla (7T), enable the visualization of the brain with very high resolution and contrast[1–3]. Positive identification of a lesion of epileptogenic potential on an MRI exam is an important component of determining the most promising treatment options for refractory epilepsy. The increased strength of the main magnetic field in 7T MRI generates a greater signal to noise ratio (SNR), which may be parlayed into enhanced conspicuity of abnormal structural features in epilepsy including those beyond the epileptogenic focus. There is increasing evidence that epilepsy is a complex network disease affecting brain functioning interictally and altering brain structure beyond the primary suspected seizure onset zone (SOZ)[4–8]. Subtle MRI features, now visible at ultra-high fields, may prove to be non-invasive biomarkers towards localizing and confirming the suspected SOZ, even when the features are not directly related to the epileptogenic focus. Perivascular spaces (PVSs), also known as Virchow-Robin spaces[9], are small cerebrospinal fluid-filled areas between blood vessels and the pia mater, and can be visualized using high resolution T_2-weighted MRI sequences[10]. The brain lacks conventional lymphatic vessels and a growing body of research suggests that PVSs play an important role in a waste clearance, or glymphatic (glial + lymphatic), system [11–15]. Recent experiments indicate the involvement of PVSs in the recruitment of macrophages across the blood brain barrier[16, 17]. Alteration in PVSs structure and appearance on high resolution MRI exams and may provide biomarkers for the altered macrophage activity associated with seizure onset[18].

Historically, PVSs have been visible on MRI only when grossly enlarged by diseases or disorders[19]. PVSs have been reported in previous investigations of epilepsy; however, the relationship between a patient's epilepsy and the presence of enlarged PVSs remains uncertain[20–23]. This has been true, in part, because even when enlarged, these spaces frequently remain below the threshold of *in vivo* detectability using MRI. Thus, in the past, smaller PVSs often had to be studied on biopsy specimens or post-mortem, and analysis may have been challenged by distortions of the physical dimensions of PVSs on *ex vivo* histological specimens. The enhanced contrast and resolution made possible by 7T MRI has enabled the noninvasive visualization and characterization of PVSs *in vivo* and high-resolution MRI experiments have begun to quantify PVSs as potential biomarkers for neurological disorders or diseases[24–26] as well as characterizing them in healthy volunteers[27]. The U.S. Food and Drug Administration has designated MR imaging scanners functioning at 8 Tesla and below as non-significant risk[1] and vendors are already building new 7T models that are slated for 510K approval. In a recent study by our group, PVSs were observed in the brains of both healthy controls and in patients with focal epilepsy, and

qualitative assessment suggested that the distributions of PVSs in the healthy controls were roughly symmetric while there was a trend towards asymmetry in the distributions of PVSs *in vivo* in epilepsy patients[28].

In this work, we performed a quantitative evaluation of the PVS distribution in epilepsy patients and healthy controls. In epilepsy patients with a localizable suspected SOZ, we also compared the asymmetric localization of PVSs to the suspected SOZ.

Methods

Subjects and Recruitment

Institutional Review Board approval was obtained before commencing subject recruitment. Written informed consent was obtained from all subjects prior to scanning. Between July 2014 and October 2016, we recruited epilepsy patients and healthy volunteers, between 18–65 years of age at the time of scanning with no contraindications to 7T MRI. Epilepsy patients were recruited through their neurologist at the Epilepsy Center at Mount Sinai Hospital and had definite focal epilepsy identified through clinical signs and electroencephalogram (EEG) data. Patients were excluded if they had had a traumatic brain injury or brain infection. All epilepsy patients were MRI-negative (no epileptogenic abnormalities identified) on previously-acquired diagnostic MRI scans. We scanned 21 subjects with focal epilepsy (13 males, 8 females, age 33 ± 11 years) and 17 healthy volunteers (11 males, 6 females, age 33 ± 9 years). The characteristics of both groups are reported in the supplemental material (Table e-1).

Axial T_2-weighted turbo spin echo (T_2 TSE) images were used for PVS tracing and quantification. Slices were defined along the plane of the anterior commissure-posterior commissure line and the acquisition volume extended from the top of the head to the cerebellum. These T_2 TSE images were obtained as part of a comprehensive epilepsy 7T imaging protocol which also included T_1-weighted and susceptibility weighted imaging sequences. T_2 TSE sequence parameters were: TR = 6000 ms, TE = 69 ms, flip angle = 150°, Field of View = 202 x 185 mm^2, matrix = 512x464, in-plane resolution 0.4 x 0.4 mm^2, slice thickness = 2 mm, slices = 40, BW = 279 Hz/pixel, time = 6:50 min. Images were acquired on a 7T whole body MRI scanner (MAGNETOM 7T, Siemens Erlangen), equipped with a SC72CD gradient coil (G_{max} = 70 mT/m and max slew rate = 200 T/m/s), using a single channel transmit and a 32-channel receive head coil (Nova Medical, Wilmington, MA).

Image Processing

Image processing on the axial T_2 TSE images was performed in Osirix (Pixmeo, Geneva) on bicubic interpolated images by a reader blinded to the status (epilepsy patient or control) of the subject. The location and cross-sectional diameter (*d*) of all PVSs in each slice were manually marked. To assist in registration and segmentation, 16 common and reproducible anatomical landmarks were identified in each subject, including 4 midline landmarks (superior vermis, highest callososeptal margin, rostrum, and splenium) and 6 bilateral structures (cortex in closest proximity to top of ear pinnae, occipital poles, frontal poles,

superior-cortex bilaterally, posterior hippocampal margins, and anterior hippocampal margins). The PVSs and anatomical landmarks, in the same coordinate axis, were exported from Osirix to custom software built in Matlab (The Mathworks, Inc., Natick, MA). Using the coordinates of the anatomical landmarks, each marked PVS was categorized as being localized in either the right or left hemisphere. The PVSs in each hemisphere were then further subdivided, based on their coordinates, into one of seven regions: 1) anterior parietal lobe, 2) posterior parietal lobe, 3) occipital lobe, 4) anterior temporal lobe, 4) posterior temporal lobe, 6) anterior frontal lobe, and 7) posterior frontal lobe.

Analysis

Each marked PVS with a diameter $d \geq 0.5$ mm was binned by hemisphere and region determined by the location of the center of the diameter measurement. Figure 1 shows a representative schematic of all the PVSs in a healthy control brain, binned by region for a sagittal projection through the brain (Figure 1A) and a sagittal-oblique representation (Figure 1B). The sum of the PVSs, weighted by the diameter, in both the left and right hemispheres for each region, j, was calculated using Equation 1.

$$S_j = \sum_{i=1}^{N_j} d_i \quad (1)$$

N_j is the total number of PVSs in region j, and d_i is the diameter of the i^{th} PVS in the region. In order to assess the distribution of PVSs in each subject, an asymmetry index (AI) was calculated using the results of Equation 1 for each hemisphere and region in Equation 2.

$$AI = \frac{S_{jr} - S_{jl}}{\frac{1}{2}(S_{jr} + S_{jl})} \quad (2)$$

In Equation 2, S_{jl} and S_{jr} are the weighted sums of the PVSs in the left and right hemispheres of the same region. The lateralization or, equivalently, the hemisphere with predominance of PVSs (i.e. higher weighted sum) was noted for each region. A positive AI reflects predominance of PVSs in the right hemisphere, while a negative AI reflects predominance of PVSs in the left hemisphere. In addition, the maximum absolute amplitude among all 7 AI's ($|AI_{max}|$) was calculated for each subject. A Mood's median test was performed to compare the $|AI_{max}|$ in epilepsy patients to healthy controls.

Additionally, clinical and electrographic data were reviewed by two epileptologists to determine the suspected hemisphere and lobe of the SOZ; a 7T MRI report was generated by consensus of two CAQ-credentialed neuroradiologists blinded to the status of the patient (epilepsy patient or healthy control). The lateralization of the PVS asymmetry in epilepsy patients was compared to the lateralization of their suspected SOZ. Finally, where the lobe or hemisphere of a suspected SOZ was identified through EEG or semiology, this region was compared to the region producing $|AI_{max}|$.

Additional Analysis

To investigate the normal distribution of PVSs, the number of PVSs visible on the T_2 TSE image was compared between healthy controls and epilepsy patients and the total number of PVSs in the brain was plotted against age.

To gain further insight into the normal regional distribution of PVSs, and assess if the PVS asymmetry was the result of a relative reduction or increase in PVSs, we calculated the relative weighted sum of PVSs ($S_{j,Rel}$) in each brain region, normalized these sums by the total number of PVSs in the whole brain.

$$S_{j,Rel} = \frac{2 * S_j}{\sum S_j} * 100\,\% \quad (3)$$

In equation 3, S_j is the sum of the PVSs in one brain region (right side or left side) while Σ S_j is the weighted sum over all regions of the brain (right hemisphere and left hemisphere). We then calculated the mean ($S_{j,Avg}$) and standard deviation of these relative values in healthy controls.

In the region of maximum asymmetry in each subject, the AI was calculated using S_{jr} and S_{jl}. To investigate the asymmetry in relation to the normal distribution of PVSs in the brain, we compared the S_{jr} and S_{jl} (relative to the total number of PVSs in the brain) in the region of maximum asymmetry in each hemisphere in both epilepsy patients and controls to $S_{j,Avg}$ for that region. In each case one side (the affected side) had a larger absolute deviation from $S_{j,Avg}$, and one side (the contralateral side) approached $S_{j,Avg}$ more closely. The normalized ratios are plotted in Figure 5.

Results

The imaging sessions were well-tolerated by the subjects and no adverse events occurred. Qualitative 7T structural imaging results and, when available, the diagnostic and therapeutic surgical outcome (Engel Class)[29] are reported in the supplemental material (Table e-2). Figure 2 shows the high-resolution T_2 TSE images obtained on two epilepsy patients. Enlarged regions in Fig. 2 highlight hyperintense PVSs and green lines indicate manually measured PVS diameters. Asymmetric PVS distribution is qualitatively visualizable in Figure 2D. The distribution of $|AI_{max}|$ among subjects is plotted in Figure 3 for epilepsy patients and controls. No significant difference was found between the total number of PVSs (n) in epilepsy patients (n = 461 – 3844, n_{avg} = 1603 ± 890) and controls (n = 533 – 4308, n_{avg} = 1902 ± 1100). The total number of PVSs visible in all subjects was positively correlated to age as shown in Figure 4. We summarized the following for each patient in Table 1: (1) patient number; (2) the side and region of the suspected SOZ; (3) the region of maximal PVS asymmetry (i.e. the region of $|AI_{max}|$); (4) the value of the AI in the maximally asymmetric region (negative values show left-dominant PVSs, while positive values show right-dominant PVSs); (5) the relationship between the SOZ and the region of |

AI_{max}|; and (6) whether asymmetry is caused by an increase or decrease in PVSs when compared to mean regional PVSs in healthy controls ($S_{j,Avg}$).

Overall Asymmetry Analysis

All subjects showed some asymmetry in the distribution of PVSs. Figure 3 is a box plot showing distribution of $|AI_{max}|$ in epilepsy patients and controls. As shown in Figure 3, the overall maximum asymmetry was higher in epilepsy patients than in healthy controls. Specifically, the median $|AI_{max}| = 0.50$ in epilepsy patients and median $|AI_{max}| = 0.34$ in healthy controls; and this difference was significant ($p = 0.016$). When comparing the weighted sum of PVSs, an $|AI_{max}|$ of 0.50 represents a factor of 1.7 difference between the left and right sides and an $|AI_{max}|$ of 0.34 represents a factor of 1.4 difference between the left and right sides.

Region of maximal PVS asymmetry and relation to suspected SOZ

In healthy controls, the region producing $|AI_{max}|$ was relatively evenly distributed between the lobes of the brain. Specifically, in healthy controls, $|AI_{max}|$ was found 5 times in the frontal lobe, and 4 times each in the temporal, occipital and parietal lobes. In the group of epilepsy patients, the regions producing $|AI_{max}|$ were more clustered, with the highest number of occurrences in the frontal lobe (8 times) and parietal lobe (8 times), then in the temporal lobe (5 times) and finally none in the occipital lobe. In 18 of the epilepsy patients, a lobe or area associated with the suspected SOZ could be identified using clinical and diagnostic data. In these subjects, this corresponded to the region producing $|AI_{max}|$ 72% of the time. Individual SOZ determinations and matches to regions of PVS asymmetry are reported in Table 1.

Analysis to determine whether PVSs are reduced or increased in asymmetric regions

Figure 5A shows the relative weighted sum of PVSs ($S_{j,Avg}$) for each region of the brain averaged over the healthy control group. Figure 5B shows relative weighted sum of PVSs ($S_{j,Rel}$) in the region of maximum asymmetry for epilepsy patients, and compares this to $S_{j,Avg}$. The black bar shows $S_{j,Rel}$ for the side of the brain deviating most from $S_{j,Avg}$ (the "affected side"), while the grey bar shows $S_{j,Rel}$ for the side contralateral to the affected side. As shown in Fig. 5B, in epilepsy patients, the affected side (black bar) often has a lower mean weighted sum of PVSs than the control group average, indicating a diminishment of PVSs within the region on this side; while the contralateral side (grey bar) generally does not exhibit any enhancement or diminishment relative to the average. Figure 5C shows the same analysis for the healthy controls. As seen in Fig. 5C, the $S_{j,Rel}$ values on both sides in maximally asymmetric regions of healthy controls do not follow the same trend as the patient group, with both black and grey bars falling above and below the regional average to a with similar frequency, and the black bars differing from $S_{j,Avg}$ to a lesser extent in healthy controls when compared to the patient group. Our data indicates that PVS asymmetry in epilepsy patients may be caused by a reduction in size and/or number of PVSs on the affected side of the brain. Table 1, columns 5 and 6 indicate when this reduction is coincident with the suspected SOZ.

Discussion

The quantitative analysis of PVS distribution performed in this study showed that greater overall PVS asymmetry exists in the brains of the epilepsy patients when compared to healthy controls (p=0.016). We also found that in the epilepsy patient group, the region of maximum asymmetry is often within the suspected SOZ (72% match), indicating that PVS distribution may be strongly linked to effects of epilepsy on the brain. A final interesting outcome of our analysis was that an apparent reduction of PVSs is causing the asymmetry in the brains of epilepsy patients when compared to controls (Figure 5).

There are a number of limitations to the current experiment. Since this study is not longitudinal, it is unclear whether structural changes are a cause or consequence of the seizures. Furthermore, imaging at a single point cannot clarify how the configuration and size of perivascular spaces might change over time. Future investigations would benefit from an analysis of PVSs across a number of time points in individuals from initial diagnosis through pre-surgical planning. In addition, absence of histopathologic specimens might also limit our understanding of the significance of PVS appearance on imaging.

The results suggest a relationship between PVS asymmetry and epilepsy. One explanation may be that PVS asymmetry is one of many effects of epilepsy on neurological structure or function. One possible mechanism for this could be disrupted macrophage activity in the SOZ. PVSs may be part of the glymphatic pathways[11, 12] and it has been reported that neuronal hyperactivity, such as seizures, can decouple the relationship between apoptosis and phagocytosis[18]. This decoupling can reduce the rate of recruitment of macrophages to break down apoptotic cells such that they remain in situ longer and are cleared, through the lymphatic system, over an extended time frame[18, 30]. Future work, involving a longitudinal analysis of PVS distribution and/or a histological analysis of resected epileptogenic tissue could confirm this effect. To our knowledge, this is the first report correlating a diminishment of PVSs in the brain with seizure onset.

In this work, we calculate right-left asymmetry in PVSs as a potential biomarker of SOZ. Physiological right-left asymmetry has been reported in multiple previous investigations of the brain[31–34]. Thus, even in healthy volunteers, perfect symmetry between hemispheres is not expected and some degree of asymmetry in the distribution of PVSs was observed in every subject scanned. However, when epilepsy patients are compared to healthy controls, without consideration of the suspected SOZ, $|AI_{max}|$ in epilepsy patients is still significantly greater than that in healthy controls.

The total number of PVSs was found to increase with age, which is consistent with prior reports[35, 36] and thought to reflect atrophy associated with aging. Figure 4 shows that both epilepsy patients and healthy controls exhibit an age-typical increase in PVSs. Figure 5 suggests that this increase in PVSs with age is decoupled from the asymmetry detected in epilepsy patients since the asymmetry is related to a regional decrease in the relative weighted sum of PVSs rather than an increased in PVSs due to brain volume loss. Previous work has also found a disproportionate increase in the number of dilated PVSs in the brains of men when compared to women in an older population [36, 37]. In our analysis, we found no

evidence confirming this gender differential, but out of caution we did control for age and gender differences. Additionally, we did not find a significant difference in the total number of PVSs identified in epilepsy patients and controls.

In our analysis, we summed the number of the PVSs, weighted by the diameter of each, to determine the PVS asymmetry and perform our quantitative analyses. It is unclear whether volumes, weighted, or unweighted numerical counts may ultimately provide the best metric of PVS quantification and analysis; indeed, all approaches are represented in the literature[37–40]. We chose to give some weight to the extent of dilation of the PVSs as suggestive of the magnitude of the physiological effect of seizures on PVSs.

The voxels in the T_2 TSE sequence used were non-isotropic: 0.4 mm x 0.4 mm in-plane with 2 mm thick slices. The high in-plane resolution of this sequence combined with the T_2 contrast, provided the best depiction of the PVSs. Since this resolution was consistent for the whole brain and for all subjects studied, it should not affect the asymmetry calculations between brain regions or statistical calculations between patient and control groups. However, an isotropic 3D T_2 weighted sequence with greater B_1 and B_0 immunity would be optimal for quantification in the future. The resolution and contrast offered at 7T enabled us to visualize many PVSs which were undetectable at lower field strengths. The threshold for analysis used in this experiment of $d \geq 0.5$ mm was chosen to produce consistent and reproducible results for marking and quantification. A $d \geq 0.5$ mm threshold resulted in roughly equivalent numbers of PVSs detected in both epilepsy patients and healthy controls of comparable age. This suggests that, while further improvement of T_2-weighted image resolution may result in the detection of more PVSs or assist in automatic processing of PVSs, it will not significantly alter the results of this analysis.

Conclusion

PVS distribution was found to be significantly more asymmetric in epilepsy patients than in healthy controls when quantified on high-resolution 7T MRI scans. In 72% of epilepsy patients studied, asymmetry was greatest in the same lobe as the suspected SOZ. Systematic quantification of PVSs at 7T could provide a valuable imaging biomarker to study the effects of epilepsy on the brain and potentially improve localization of SOZ for surgical planning.

Supplementary Material

Refer to Web version on PubMed Central for supplementary material.

Acknowledgments

Funding

The research reported in the manuscript was supported by NIH-NINDS R00 NS070821; NIH R01 MH109544; Health Resources and Services Administration Health Careers Opportunity Program: Northeast Regional Alliance MedPREP Program, Icahn School of Medicine at Mount Sinai Grant D18HP29036; Icahn School of Medicine Capital Campaign; Translational and Molecular Imaging Institute and Department of Radiology, Icahn School of Medicine at Mount Sinai; Siemens Healthcare.

References

1. Balchandani P, Naidich TP. Ultra-High-Field MR Neuroimaging. AJNR Am J Neuroradiol. 2015; 36:1204–1215. [PubMed: 25523591]
2. Duyn JH. The future of ultra-high field MRI and fMRI for study of the human brain. Neuroimage. 2012; 62:1241–1248. [PubMed: 22063093]
3. Springer E, Dymerska B, Cardoso PL, et al. Comparison of Routine Brain Imaging at 3 T and 7 T. Invest Radiol. 2016; 51:469–482. [PubMed: 26863580]
4. Gilmore R, Morris H 3rd, Van Ness PC, et al. Mirror focus: function of seizure frequency and influence on outcome after surgery. Epilepsia. 1994; 35:258–263. [PubMed: 8156943]
5. Goldensohn ES. The relevance of secondary epileptogenesis to the treatment of epilepsy: kindling and the mirror focus. Epilepsia. 1984; 25(Suppl 2):S156–173. [PubMed: 6430692]
6. Kim J, Shin HK, Hwang KJ, et al. Mirror focus in a patient with intractable occipital lobe epilepsy. J Epilepsy Res. 2014; 4:34–37. [PubMed: 24977131]
7. Ahmadi ME, Hagler DJ Jr, McDonald CR, et al. Side matters: diffusion tensor imaging tractography in left and right temporal lobe epilepsy. AJNR Am J Neuroradiol. 2009; 30:1740–1747. [PubMed: 19509072]
8. Szaflarski JP, Gloss D, Binder JR, et al. Practice guideline summary: Use of fMRI in the presurgical evaluation of patients with epilepsy: Report of the Guideline Development, Dissemination, and Implementation Subcommittee of the American Academy of Neurology. Neurology. 2017; 88:395–402. [PubMed: 28077494]
9. Kwee RM, Kwee TC. Virchow-Robin spaces at MR imaging. Radiographics. 2007; 27:1071–1086. [PubMed: 17620468]
10. Tsitouridis I, Papaioannou S, Arvaniti M, et al. Enhancement of robin-virchow spaces MRI evaluation. Neuroradiol J. 2008; 21:490–499. [PubMed: 24256953]
11. Esiri MM, Gay D. Immunological and neuropathological significance of the Virchow-Robin space. J Neurol Sci. 1990; 100:3–8. [PubMed: 2089138]
12. Bakker EN, Bacskai BJ, Arbel-Ornath M, et al. Lymphatic Clearance of the Brain: Perivascular, Paravascular and Significance for Neurodegenerative Diseases. Cell Mol Neurobiol. 2016; 36:181–194. [PubMed: 26993512]
13. Aribisala BS, Wiseman S, Morris Z, et al. Circulating inflammatory markers are associated with magnetic resonance imaging-visible perivascular spaces but not directly with white matter hyperintensities. Stroke. 2014; 45:605–607. [PubMed: 24399375]
14. Ramirez J, Berezuk C, McNeely AA, et al. Imaging the Perivascular Space as a Potential Biomarker of Neurovascular and Neurodegenerative Diseases. Cell Mol Neurobiol. 36:289–299.
15. Jessen NA, Munk AS, Lundgaard I, et al. The Glymphatic System: A Beginner's Guide. Neurochem Res. 40:2583–2599.
16. Bechmann I, Priller J, Kovac A, et al. Immune surveillance of mouse brain perivascular spaces by blood-borne macrophages. Eur J Neurosci. 2001; 14:1651–1658. [PubMed: 11860459]
17. Corraliza I. Recruiting specialized macrophages across the borders to restore brain functions. Front Cell Neurosci. :8.
18. Abiega O, Beccari S, Diaz-Aparicio I, et al. Neuronal Hyperactivity Disturbs ATP Microgradients, Impairs Microglial Motility, and Reduces Phagocytic Receptor Expression Triggering Apoptosis/Microglial Phagocytosis Uncoupling. PLoS Biol. 2016; 14:e1002466. [PubMed: 27228556]
19. Groeschel S, Chong WK, Surtees R, et al. Virchow-Robin spaces on magnetic resonance images: normative data, their dilatation, and a review of the literature. Neuroradiology. 2006; 48:745–754. [PubMed: 16896908]
20. Betting LE, Mory SB, Lopes-Cendes I, et al. MRI reveals structural abnormalities in patients with idiopathic generalized epilepsy. Neurology. 2006; 67:848–852. [PubMed: 16966549]
21. Song CJ, Kim JH, Kier EL, et al. MR imaging and histologic features of subinsular bright spots on T2-weighted MR images: Virchow-Robin spaces of the extreme capsule and insular cortex. Radiology. 2000; 214:671–677. [PubMed: 10715028]

22. Saito Y, Sasaki M, Hanaoka S, et al. A case of Noonan syndrome with cortical dysplasia. Pediatr Neurol. 1997; 17:266–269. [PubMed: 9390707]
23. Boxerman JL, Hawash K, Bali B, et al. Is Rolandic epilepsy associated with abnormal findings on cranial MRI? Epilepsy Res. 2007; 75:180–185. [PubMed: 17624735]
24. Cai K, Tain R, Das S, et al. The feasibility of quantitative MRI of perivascular spaces at 7T. J Neurosci Methods. 2015; 256:151–156. [PubMed: 26358620]
25. Bouvy WH, Zwanenburg JJ, Reinink R, et al. Perivascular spaces on 7 Tesla brain MRI are related to markers of small vessel disease but not to age or cardiovascular risk factors. J Cereb Blood Flow Metab. 2016; 36:1708–1717. [PubMed: 27154503]
26. Kilsdonk ID, Steenwijk MD, Pouwels PJ, et al. Perivascular spaces in MS patients at 7 Tesla MRI: a marker of neurodegeneration? Mult Scler. 2015; 21:155–162. [PubMed: 25013150]
27. Zong X, Park SH, Shen D, et al. Visualization of perivascular spaces in the human brain at 7T: sequence optimization and morphology characterization. Neuroimage. 2016; 125:895–902. [PubMed: 26520772]
28. Feldman RE, Dyvorne HA, Delman BN, et al. 7T Imaging of patients with focal epilepsy who appear non-lesional in diagnostic 1.5T and 3T MRI scans: first results. Proceedings of the Annual Meeting of the International Society for Magnetic Resonance in Medicine Toronto, Ontario, Canada. 2015:0755.
29. Engel, J, Jr. Update on surgical treatment of the epilepsies. Neurology; Summary of the Second International Palm Desert Conference on the Surgical Treatment of the Epilepsies; 1992; 1993. p. 1612-1617.
30. Diaz-Aparicio I, Beccari S, Abiega O, et al. Clearing the corpses: regulatory mechanisms, novel tools, and therapeutic potential of harnessing microglial phagocytosis in the diseased brain. Neural Regen Res. 2016; 11:1533–1539. [PubMed: 27904472]
31. Watkins KE, Paus T, Lerch JP, et al. Structural asymmetries in the human brain: a voxel-based statistical analysis of 142 MRI scans. Cereb Cortex. 2001; 11:868–877. [PubMed: 11532891]
32. Jack CR Jr, Twomey CK, Zinsmeister AR, et al. Anterior temporal lobes and hippocampal formations: normative volumetric measurements from MR images in young adults. Radiology. 1989; 172:549–554. [PubMed: 2748838]
33. Jensen BH, Hougaard A, Amin FM, et al. Structural asymmetry of cortical visual areas is related to ocular dominance. Neuroreport. 2015; 26:1071–1076. [PubMed: 26509548]
34. Cherbuin N, Luders E, Chou YY, et al. Right, left, and center: how does cerebral asymmetry mix with callosal connectivity? Hum Brain Mapp. 2013; 34:1728–1736. [PubMed: 22419524]
35. Zhu YC, Dufouil C, Mazoyer B, et al. Frequency and location of dilated Virchow-Robin spaces in elderly people: a population-based 3D MR imaging study. AJNR Am J Neuroradiol. 2011; 32:709–713. [PubMed: 21349956]
36. Zhu YC, Tzourio C, Soumare A, et al. Severity of dilated Virchow-Robin spaces is associated with age, blood pressure, and MRI markers of small vessel disease: a population-based study. Stroke. 2010; 41:2483–2490. [PubMed: 20864661]
37. Ramirez J, Berezuk C, McNeely AA, et al. Visible Virchow-Robin spaces on magnetic resonance imaging of Alzheimer's disease patients and normal elderly from the Sunnybrook Dementia Study. J Alzheimers Dis. 2015; 43:415–424. [PubMed: 25096616]
38. Wuerfel J, Haertle M, Waiczies H, et al. Perivascular spaces--MRI marker of inflammatory activity in the brain? Brain. 2008; 131:2332–2340. [PubMed: 18676439]
39. Wang X, del Valdes Hernandez MC, Doubal F, et al. Development and initial evaluation of a semi-automatic approach to assess perivascular spaces on conventional magnetic resonance images. J Neurosci Methods. 2016; 257:34–44. [PubMed: 26416614]
40. del Hernandez MC, Piper RJ, Wang X, et al. Towards the automatic computational assessment of enlarged perivascular spaces on brain magnetic resonance images: a systematic review. J Magn Reson Imaging. 2013; 38:774–785. [PubMed: 23441036]

Highlights

- The perivascular spaces were asymmetric in epilepsy patients when compared to controls ($p = 0.016$)
- 72% of patients had maximum asymmetry in the same lobe as the suspected seizure onset zone
- Detectable perivascular spaces were decreased in regions of maximum asymmetry

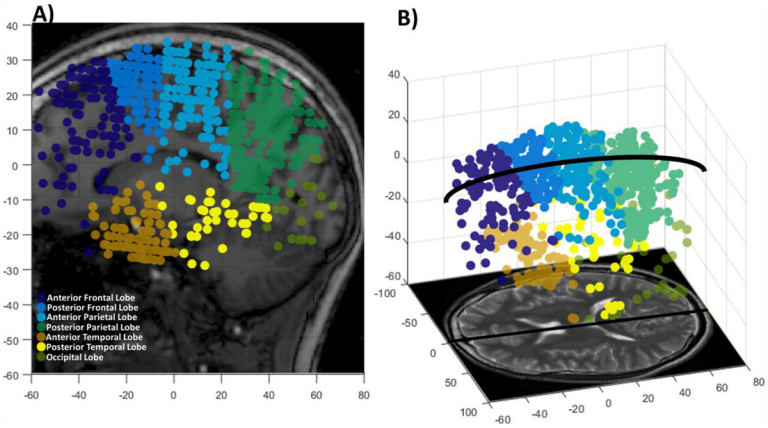

Figure 1.

Distribution of perivascular spaces (PVSs) in a healthy volunteer. Each PVS was marked, and its coordinates and diameter were recorded. The PVSs were binned into 7 different regions illustrated in A) a sagittal projection of all marked PVSs and B) and sagittal-oblique view showing the PVSs. Note: Circular markers are illustrative of the location and number of PVSs and not representative of PVS diameter. (color, 1 column)

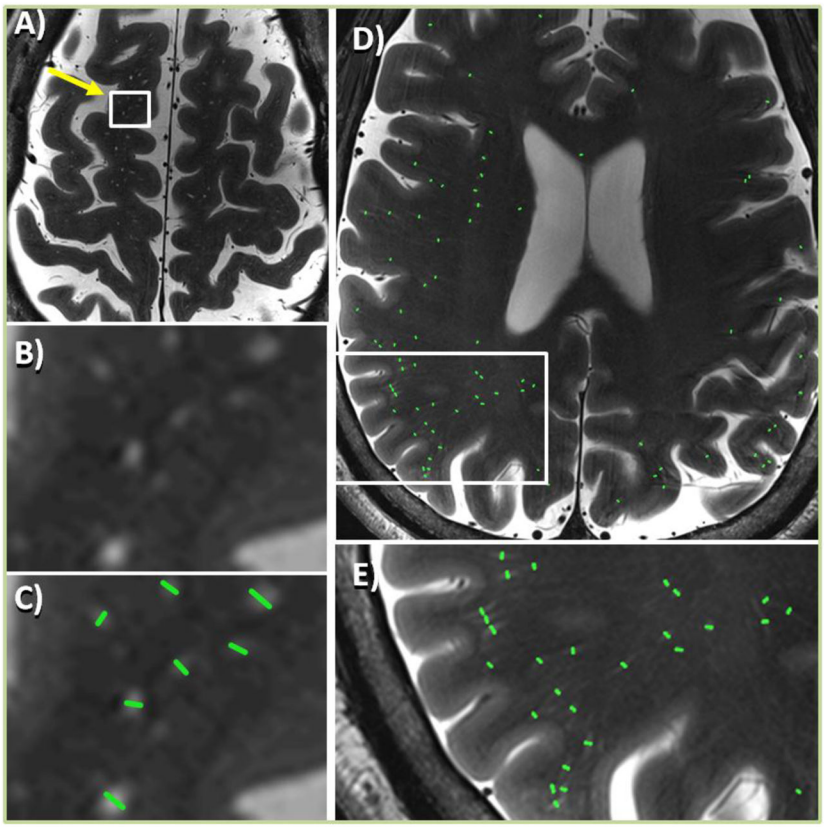

Figure 2.

Axial T_2 TSE images showing perivascular spaces (PVSs) in two epilepsy patients (A–C and D–E). A) PVSs appear as small hyperintense features in the T_2 TSE image of an epilepsy patient. B) Enlarged view of area containing PVSs for image in A; C) marked PVSs for same area as B. D) All marked PVSs in a single slice for an another epilepsy patient with high PVS asymmetry. E) Enlarged area showing marked region with predominance of PVSs when compared to contralateral side. (color, 1.5 column)

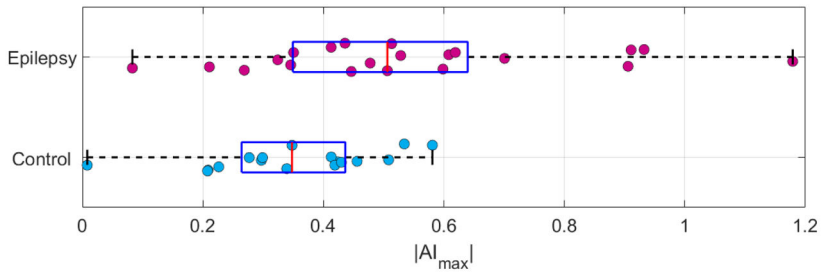

Figure 3.

Box plots of $|AI_{max}|$ distribution in epilepsy patients and controls. The whiskers span the range of the data, the blue box contains the second and third quartile, and the red bar indicates the median. Epilepsy patients have significantly higher degree of asymmetry in the region of maximal asymmetry than controls. (color, 1 column)

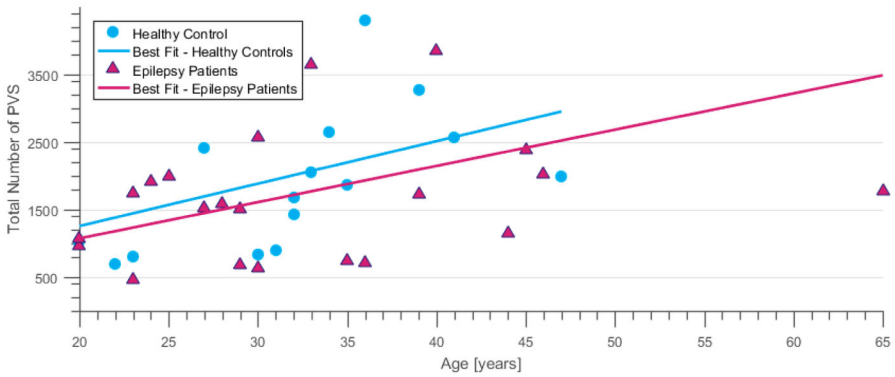

Figure 4.

Age correlation to total number of PVSs. The total number of PVSs in the brain (including SOZ and contralateral to the SOZ) plotted against the age of the subject at scan time. Although the number of PVSs is highly variable, there is a positive correlation with increasing age. (color, 1 column)

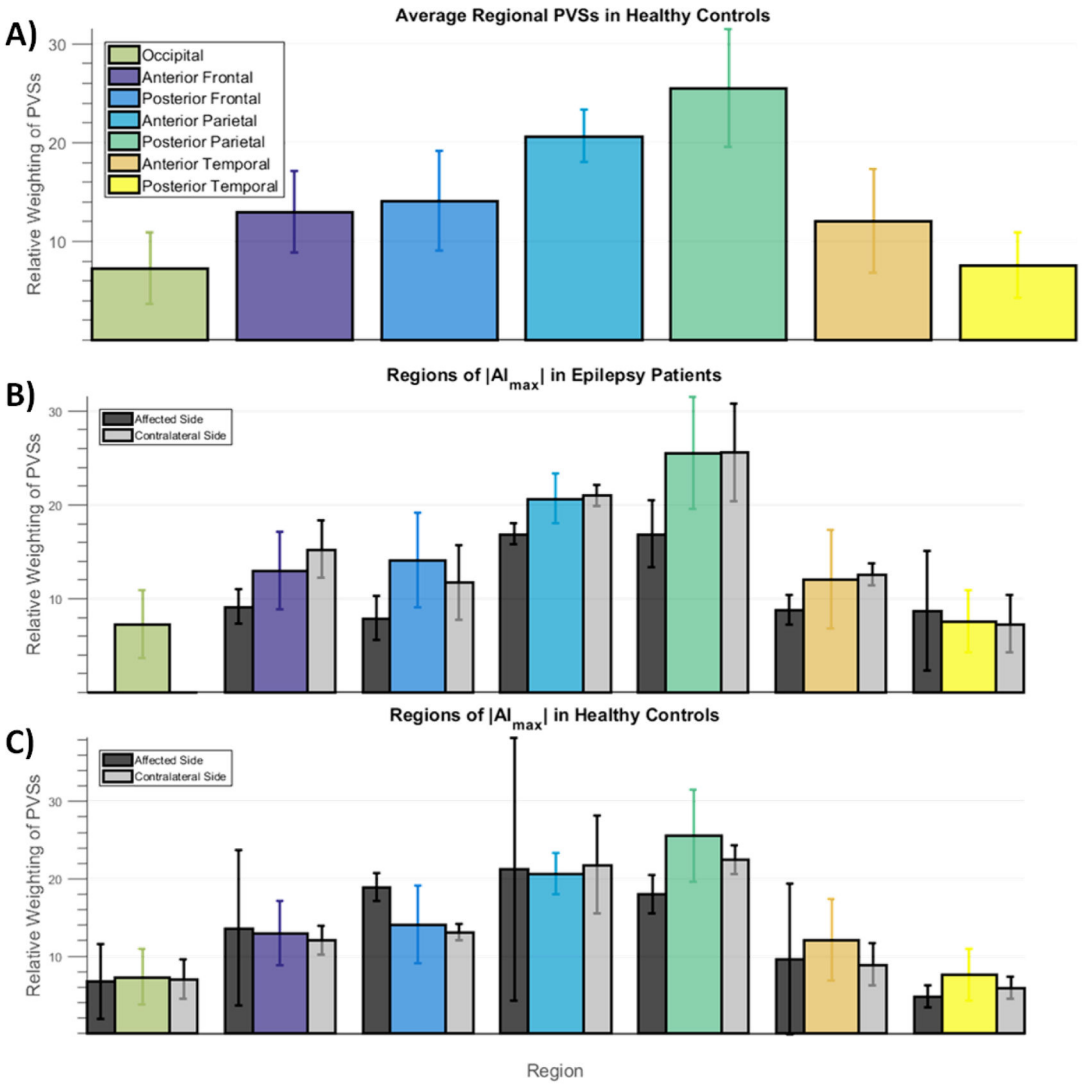

Figure 5.

Analysis of average regional PVSs in brain regions and a comparison to regions of maximum asymmetry. A) Bar graph showing average weighted sum of PVSs ($S_{j,Avg}$) in each region of the brain for the healthy control group. Values are averaged between sides. Error bars show standard deviation. B) Bar graph showing the relative weighted sum of PVSs ($S_{j,Rel}$), in regions of maximal asymmetry ($|AI_{max}|$) in the epilepsy group. Black bars show weighted sum of PVSs on the affected side, side deviating most from the average value ($S_{j,Avg}$); grey bars show weighted sum of PVSs on the contralateral side; colored bars are the average values ($S_{j,Avg}$) transposed from A) for comparison. The weighted sum of PVSs on the affected side (black bars in B) often fall below the average value, indicating that asymmetry of PVSs in the epilepsy group is often due to the diminishment or reduction of PVSs on the affected side. PVSs on the contralateral side (grey bars) hovered around average. Bar graph in C) shows the same values for the control group. No such trend towards

reduction or increase of PVSs as the source of asymmetry was observed in the control group. (color, 1 column)

Table 1

Table listing for (1) all 21 epilepsy patients: (2) the suspected seizure onset zone (SOZ); (3) the region of maximum asymmetry ($|AI_{max}|$); (4) the value of AI in the region of $|AI_{max}|$; (5) the relationship between the region of $|AI_{max}|$ and the suspected SOZ; and (6) whether PVS asymmetry is caused by an increase or decrease in PVSs in the region of $|AI_{max}|$ when compared to the regional average in controls ($S_{j,Avg}$). N/A -> indicates that no suspected SOZ was identified using clinical indications and could not be compared to the region of $|AI_{max}|$; Non Lat -> Non Lateralizable; Match -> indicates that the suspected SOZ is a match to the region of $|AI_{max}|$; No Match -> indicates that the suspected SOZ is not a match to the region of $|AI_{max}|$.

(1) ID	(2) Suspected SOZ		(3) Region of $\|AI_{max}\|$	(4) AI value in Region of $\|AI_{max}\|$	(5) SOZ vs Region of $\|AI_{max}\|$	(6) (I)ncrease or (D)ecrease S_j relative to $S_{j,Avg}$
1	Left	Temporal	Posterior Temporal	−0.2687	Match	D
2	Left	Parietal	Posterior Parietal	0.6191	Match	D
3	Left	Frontal/Temporal	Posterior Parietal	0.5985	No Match	D
4	Left	Anterior Temporal	Posterior Frontal	0.3457	No Match	D
5	Non Lat	Frontal	Anterior Frontal	0.9323	Match	D
6	Right	Temporal	Posterior Temporal	0.9057	Match	D
7	Left	Unknown	Anterior Parietal	0.083	N/A	D
8	Left	Temporal	Anterior Temporal	−0.4129	Match	I
9	Left	Unknown	Anterior Parietal	0.3241	N/A	D
10	Left	Frontal	Anterior Frontal	−0.4463	Match	D
11	Right	Frontal/Temporal	Anterior Frontal	−0.5062	Match	D
12	Left	Anterior Temporal	Anterior Frontal	−0.2108	No Match	D
13	Non Lat	Unknown	Posterior Parietal	0.5133	N/A	D
14	Right	Frontal/Parietal	Anterior Frontal	−0.4358	Match	D
15	Right	Frontal/Temporal	Posterior Parietal	1.179	No Match	D
16	Left	Parietal	Posterior Parietal	0.9108	Match	D
17	Left	Frontal/Temporal	Posterior Frontal	−0.3505	Match	D
18	Non Lat	Frontal/Temporal	Anterior Parietal	0.608	No Match	D
19	Left	Frontal/Temporal	Posterior Frontal	0.7007	Match	D
20	Left	Temporal	Anterior Temporal	−0.5283	Match	I
21	Non Lat	Anterior Temporal	Anterior Temporal	−0.4777	Match	D